Coverage and Rate Trends in Dense Urban mmWave Cellular Networks

Mandar N. Kulkarni, Sarabjot Singh and Jeffrey G. Andrews

***Abstract*—The use of dense millimeter wave (mmWave) cellular networks with highly directional beamforming stands as an intriguing solution to the current spectrum congestion problem. Due to significantly different propagation characteristics at such high frequencies, however, the coverage and rate trends differ drastically from conventional microwave networks. This paper aims to gain insights into the coverage and rate performance of mmWave cellular networks in major metropolitan cities. Our results confirm that, unlike conventional cellular networks, mmWave networks operating at 73 GHz carrier frequency are pre-dominantly noise-limited. Though larger system bandwidth leads to higher peak rates, it does not improve the cell edge rates. It is observed that dense base station (BS) deployment is the key to achieve both better coverage and rates in mmWave cellular networks. Further, based on actual building locations, we show the inadequacy of existing blockage models and validate a better blockage model.**

I. Introduction

The extensive adoption of smartphones and the maturity of corresponding application ecosystem has led to well-documented and prolific increases in wireless traffic [1]. This ongoing traffic surge has been primarily been handled so far with increased long-term evolution (LTE) deployments, small cell densification, and increased offloading, but to meet the projected needs by the end of the decade, it is plain that large amounts of new spectrum will be needed. The only place where nontrivial amounts of inactive or very lightly used spectrum can be found are above 20 GHz. Although mmWave frequencies (20-300 GHz) have long been considered attractive for indoor and personal area networks [2], [3], the large propagation losses (particularly due to near-field losses and blocking) and the expense and power-consumption of mmWave hardware had kept it from serious consideration as a cellular technology. This began to change largely due to an initiative by Samsung to seriously test this conventional wisdom [4].

Since then, the investigations in [5]–[8] have demonstrated the ability to overcome mmWave's large propagation losses using highly directional steerable antennas and beamforming, to achieve a transmission range of about 150-200 meters. The system-level simulation studies in [9]–[11] have demonstrated that dense mmWave cellular networks employing antennas with high gains and narrow beams have the potential of achieving multi-fold improvement in data rates as compared to the current LTE networks. The advancements in manufacturing low cost mmWave chips [12], [13] further strengthen the position of mmWave frequency bands as contenders for next generation cellular technology.

Prior works in [9]–[11], [14]–[16] have identified some fundamentally new coverage and rate trends exhibited by mmWave cellular networks, as compared to the conventional ones. The simulation studies in [9] showed that the thermal noise power is comparable to or even larger than the interference power, highlighting the noise-limited nature of these networks – unlike urban microwave networks which are strongly interference-limited. A similar observation was made in the analytical study in [16]. In [9], [10], it was observed that due to the power-limited nature of the cell edge users, the improvement in cell edge rates is not very high as compared to the current LTE networks. System simulations in [11] and analytical studies in [15], [16] demonstrate the importance of network densification and use of large antenna arrays for achieving high data rates in mmWave cellular networks. In [9]–[11], curve fitting techniques were employed to derive blockage models based on data obtained from experimental or ray tracing studies, which severely limits the flexibility to use these models for predicting system performance in any other urban region without performing an elaborate experimental or ray tracing study of that region. An exponential decay blockage model based on random shape theory was proposed in [17] and used in the analysis of millimeter wave networks in [14]. A LOS ball approximation to model blockages was proposed in [15], in order to simplify the analysis. However, this approximation was not validated using actual blockage scenarios. As will be demonstrated in Section IV, the coverage estimates are highly sensitive to the choice of blockage models due to the significantly different path loss for line-of-sight (LOS) and non-line-of-sight (NLOS) links. Thus, one of the main challenges in analyzing the performance of mmWave cellular networks is to accurately model blockages in the environment.

As buildings are the main source of blockage in outdoor urban environments, we use the actual building locations in two major metropolitan regions (Manhattan and Chicago) in order to incorporate urban blockage effects in our simulation study. In this work, we highlight the noise-limited nature of mmWave cellular networks operating at 73 GHz, where achieving higher peak data rates is dependent on dense BS deployment and large system bandwidth. Further, we observe that dense BS deployment is also required to improve the cell edge rates while increasing the bandwidth has minimal impact. We show the inadequacy of existing blockage models to closely track the coverage obtained using real building locations and validate a simple blockage model, proposed in [16], that captures these trends better.

This work has been supported by Nokia. The authors are with the Wireless Networking and Communication Group, The University of Texas at Austin. (email: mandar.kulkarni@utexas.edu, sarabjot@utexas.edu, jandrews@ece.utexas.edu)

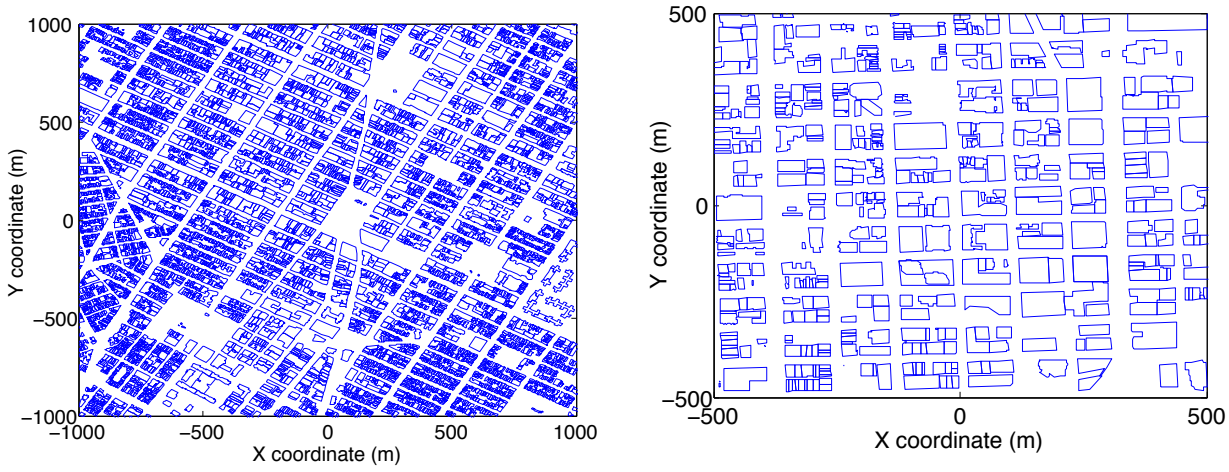

(a) Manhattan

(b) Chicago

Fig. 1: Urban areas under consideration

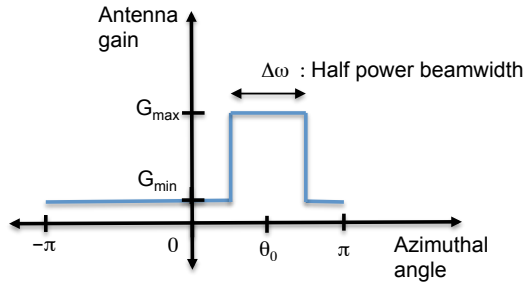

Fig. 2: Sectorized approximation to beam pattern [18]

TABLE I: Building statistics of the urban areas under consideration

Urban area	% area covered by buildings	Avg. building area (m^2)	Avg. building perimeter (m)
Chicago	42.02	886.46	114.48
Manhattan	45.83	312.26	73.78

II. System Model

We use the building locations from lower Manhattan [19] and Chicago downtown [20] regions, as shown in Fig. 1, for incorporating urban blockage effects in our simulation study. The Manhattan and Chicago regions have centroids with coordinates (40.735557^o N, 73.991527^o W) and (41.893694^o N, 87.628056^o W), respectively. The building statistics of these regions are summarized in Table I. Detailed building locations are available as usable MAT files in [21], along with the corresponding code for converting shapefiles from [19], [20] into MAT files. Consider mmWave cellular networks deployed in these regions, operating at frequency f_c with bandwidth B. We focus on outdoor downlink scenario in this work. The location of a typical outdoor user, whose performance is to be evaluated, is averaged over the 1 km $\times$ 1 km square centered at the origin of the Manhattan region. Similarly, we average the user location over the 500 m $\times$ 500 m square centered at the origin of the Chicago region. Remaining users and BSs are distributed uniformly over the entire Manhattan and Chicago regions, with densities ν users/km^2 and μ BSs/km^2. Although the users are distributed only in the outdoor region, BSs may lie inside a polygon representing a building. We assume even such BSs to be outdoors, emulating a *rooftop* location. However, we ignore 3D distances and elevation beamforming. A link is assumed to be NLOS if a building blocks the line segment joining the user and the BS, or if the BS is in a *rooftop* location.

Consider a BS at location R with respect to the user under consideration. The power received by the user from this BS is modelled as

$$\mathrm{P}_r(R,\theta) = \left(\frac{\lambda_c}{4\pi}\right)^2 \frac{\mathrm{P}_t G(\theta)}{L(R)}, \tag{1}$$

where P_t is the transmit power, λ_c is the carrier wavelength and $L(R)$ is the path loss, respectively. θ denotes the azimuthal angle of the BS beam alignment and $G(.)$ denotes the transmit antenna gain. The variation of antenna beam pattern over the elevation angle is neglected in this work. Users are assumed to be omni-directional.

The angle θ is measured with respect to the beam alignment that gives the maximum received signal power, say θ_0. For a LOS link, θ_0 is the slope of the line joining the BS-user pair under consideration. On the other hand, for a NLOS link θ_0 may be some other angle which is dependent on the geography of the region. We assume a sectorized approximation to the beam pattern, as shown in Fig. 2. The transmitter beam is said to be perfectly aligned if $\theta \in [\theta_0 - \frac{\Delta\omega}{2}, \theta_0 + \frac{\Delta\omega}{2}]$, where $\Delta\omega$ is the half power beamwidth. A perfectly aligned transmitter beam has gain $G_{\max}$, whereas a misaligned beam has gain $G_{\min}$. In this work, we assume that the beam of a BS is perfectly aligned with the user it is serving. For an interfering link, the azimuthal angle of the BS is assumed to be uniformly distributed between $-\pi$ to π. Let us denote the total antenna gain of an interfering link by ψ. Note that ψ

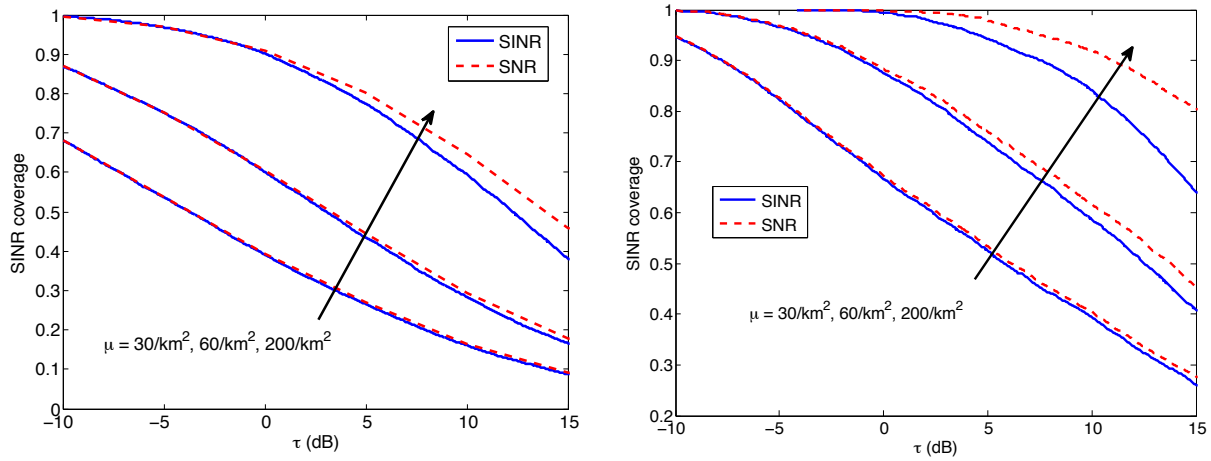

(a) B = 2 GHz. (b) B = 200 MHz.

Fig. 3: SINR coverage for Manhattan region, $\mu = 30/\text{km}^2$.

TABLE II: Simulation parameters

Parameter	Value	Parameter	Value
f_c	73 GHz	B	2 GHz
P_t	30 dBm	NF	10 dB
ν	200/ km^2	$\Delta\omega$	10^o
$G_{\max}$	18 dB	$G_{\min}$	-2 dB
α_L	2.1	α_N	3.3
Std(χ_L)	4.9	Std(χ_N)	7.6

is a Bernoulli random variable that takes value $G_{\max}$ with probability $\Delta\omega/2\pi$ and $G_{\min}$ with probability $1-\Delta\omega/2\pi$, where $\Delta\omega$ is in radians.

The path loss $L(R)$, in dB, is modelled as [10], [11]

$$L(R) = \begin{cases} 10\alpha_L \log_{10}(||R||) + \chi_L & \text{if link is LOS} \\ 10\alpha_N \log_{10}(||R||) + \chi_N & \text{otherwise,} \end{cases} \quad (2)$$

where $\{\alpha_L, \alpha_N\}$ are the path loss exponents and $\{\chi_L, \chi_N\}$ are zero mean log normal shadow fading random variables for LOS and NLOS links, respectively.

Let us denote the signal to noise ratio, the signal to interference ratio and the signal to interference plus noise ratio by SNR, SIR and SINR, respectively. Let Φ be the point process of BSs in a X-Y plane, with the user under consideration at the origin. A user is assumed to associate with the BS having smallest $L(.)$. It is assumed that the users connected to a BS are multiplexed via time division multiple access (TDMA), so that the thermal noise is collected over the entire system bandwidth. Given that the user at origin is served by a BS at location R, the SINR of the user is given as

$$\texttt{SINR} = \frac{\mathrm{P}_t G_{\max}}{\sum_{X\in\Phi, X\neq R} \frac{\mathrm{P}_t \psi_X L(R)}{L(X)} + \left(\frac{4\pi}{\lambda_c}\right)^2 \sigma^2 L(R)}, \quad (3)$$

where the random variables ψ_X are independently and identically distributed to ψ. The noise power (in dB) is calculated as $\sigma^2 = -174$ dBm/Hz$+10\log_{10}$(B Hz)$+$NF dB, where NF is the noise figure in dB. Downlink rate (in bits per second) of the user connected to a BS serving a total of N users is [22]

$$\text{Rate} = \frac{\mathrm{B}}{N}\log_2(1+\texttt{SINR}), \quad (4)$$

The SINR and rate coverage for thresholds τ and τ_r are defined as $\mathbb{P}(\texttt{SINR} > \tau)$ and $\mathbb{P}(\text{Rate} > \tau_r)$, respectively.

The simulation parameters are based on previous studies including [4], [8], [11] and are given in Table II. Here, Std(.) is the standard deviation of a random variable. The user location is averaged over 5000 drops, unless specified otherwise.

III. Coverage and Rate Trends

The complementary cumulative distribution functions (CCDF) of SINR and SNR for the Manhattan region is shown in Fig. 3. As is evident from Fig. 3(a), for B = 2 GHz, the SINR and SNR distributions are very close to each other even for ultra dense networks with $\mu = 200/\text{km}^2$, thereby highlighting the minimal impact of interference on coverage. This is unlike the conventional microwave cellular case, where SIR $\approx$ SINR. Fig. 3(b) further elaborates on this insight. We observe that the noise power still plays a dominant role in the SINR performance for moderately dense networks, even if we decrease the bandwidth to 200 MHz. However, interference effects start becoming notable for very large μ in this case. Fig. 3 also shows that increasing μ improves the coverage. The probability of connecting to a BS having lower path loss increases with μ, thereby increasing the probability of having higher desired signal power. Although the received interference power also increases with μ, SINR coverage improves due to the noise-limited nature of the system. Since designing noise-limited systems is much easier than interference-limited systems, it would be beneficial to find alternative techniques to improve coverage (like choosing larger antenna arrays at BSs [11]), which can be used in conjunction with increasing μ, for networks with moderate bandwidth (in the order of MHz).

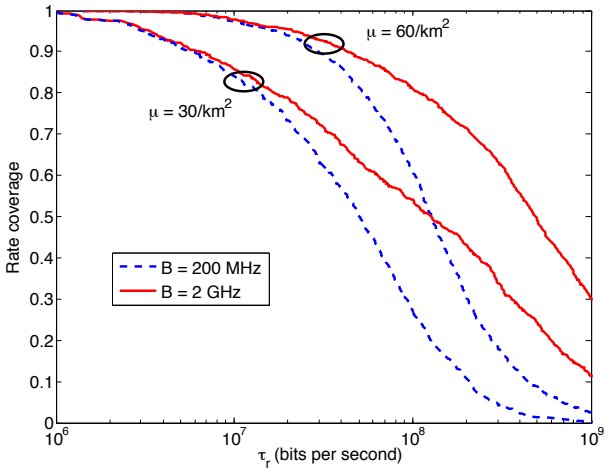

Fig. 4: Effect of bandwidth and BS density on the rate coverage for Manhattan region.

The effect of B and μ on rate coverage is shown in Fig. 4. From the figure, we observe that increasing B increases the probability of achieving high data rates in the order of Gbps. However, it is interesting to note that increasing B from 200 MHz to 2 GHz does not significantly improve the rate coverage for lower thresholds, which represent the cell edge rates. As the cell edge users are power limited, they experience very low SINR and thus increasing B has negligible impact on rate. On the contrary, increasing μ not only reduces the path loss to the serving BS but also the number of users served per BS. Thus, increasing μ increases the data rates, including cell edge rates, as shown in Fig. 4. Similar insights on SINR and rate coverage were observed for the Chicago region but are not shown here due to space constraints.

In the next section, we compare the SINR coverage obtained using existing blockage models with that obtained using actual building locations.

IV. Blockage Models for mmWave Cellular Networks

In this section, we compare the following blockage models for $\mu = 30/\text{km}^2$, with SINR coverage as the comparison metric:

- 3GPP urban outdoor micro-cellular model [23]: In this model,
$$\mathrm{p_L}(x) = \min\left(18/x, 1\right)\left(1 - e^{-x/36}\right) + e^{-x/36}, \quad (5)$$
where $\mathrm{p_L}(x)$ is the probability that a link of length x is LOS.
- Random shape theory model [17]: For randomly distributed outdoor users and indoor/outdoor BSs, $\mathrm{p_L}(x) = \exp(-\beta x)$[1], where β is the blockage parameter given by
$$\beta = \frac{-\rho \ln(1-\kappa)}{\pi A}, \quad (6)$$
where κ is % area covered by buildings, ρ is the average building perimeter and A is the average building area. Based on the values of these parameters given in Table I, β is found to be 0.046 for the Manhattan region and 0.022 for the Chicago region.
- LOS ball model 1 [15]: In this model,
$$\mathrm{p_L}(x) = \begin{cases} 1 & \text{if } x < \mathrm{D_0} \\ 0 & \text{otherwise.} \end{cases} \quad (7)$$
In order to compare this model, $\mathrm{D_0}$ is found by matching the LOS association probability ($\mathrm{A_L}$) found from system simulations with $1 - \exp\left(-\pi\mu \mathrm{D_0^2}\right)$ [15]. The values of $\mathrm{D_0}$ are found to be 77.2m and 76.17m for the Manhattan and Chicago regions, respectively.
- LOS ball model 2 [15]: In this model, $\mathrm{p_L}(x)$ is same as equation (7). However, $\mathrm{D_0}$ is chosen such that the mean number of LOS BSs ($\mathrm{M_L}$), visible to the user under consideration, is matched. The corresponding values of $\mathrm{D_0}$ are found to be 90.42 m and 87.13 m for the Manhattan and Chicago regions, respectively.

For simulating the SINR coverage using these blockage models, we follow the same procedure as given in Section II, except that the blockage models are used to decide LOS/NLOS instead of actual buildings and averaging of the user and BS locations is done over a larger region, 5 km by 5 km square centred at the user under consideration. As is evident from the figures, the 3GPP blockage model gives an optimistic estimate to the SINR coverage. It can be seen that the exponential decay model [17] gives a close estimate to the coverage for Chicago region, whereas it gives a conservative estimate for the Manhattan region. Note that although the SINR coverage obtained for the Manhattan and Chicago regions are comparable to each other[2], the estimates of β using equation (6) are notably different. The SINR coverage obtained using both the LOS ball models [15] have a prominent flat region in the threshold range of -10 dB to 10 dB, which deviates from the SINR distribution obtained using actual building locations. The above observations stem the need for a better blockage model.

Consider the blockage model proposed in [16], with $\mathrm{p_L}(x)$ given by
$$\mathrm{p_L}(x) = \begin{cases} \mathrm{C} & \text{if } x \le \mathrm{D} \\ 0 & \text{otherwise,} \end{cases} \quad (8)$$
for some $0 \le \mathrm{C} \le 1$ and $\mathrm{D} > 0$. Note that the LOS ball model is a special case of this model, where $\mathrm{C} = 1$ and the value of D is derived by matching either $\mathrm{A_L}$ or $\mathrm{M_L}$. Choosing D based on matching $\mathrm{A_L}$ makes the blockage model dependent on the BS density and the channel model. Although, choosing D based on matching $\mathrm{M_L}$ makes the model independent of the channel model [15], Fig. 5 motivates the need to refine in the choice of (C, D) pair.

As described in [16], we estimate C empirically by equating it to the average LOS fractional area in a ball of

[1]This expression holds only for link lengths greater than a particular threshold. However, since a closed form solution does not exist for link lengths smaller than the threshold, the expression $\exp(-\beta x)$ is used for all link lengths, as is also done in [17].

[2]It so happens that the coverage in these two regions is very close to each other, for the system model described in Section II. No general claim is being made here.

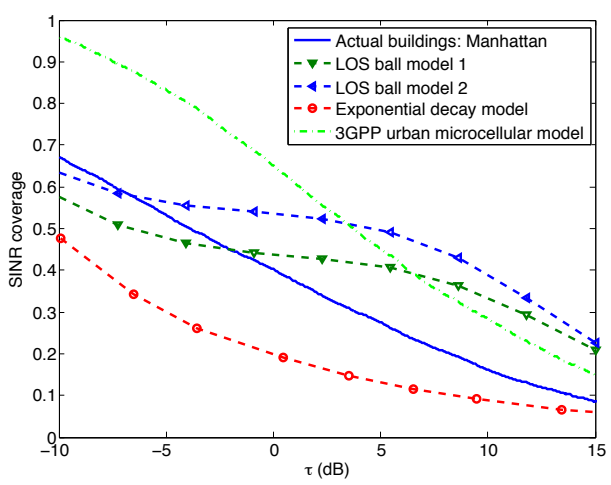

(a) Manhattan

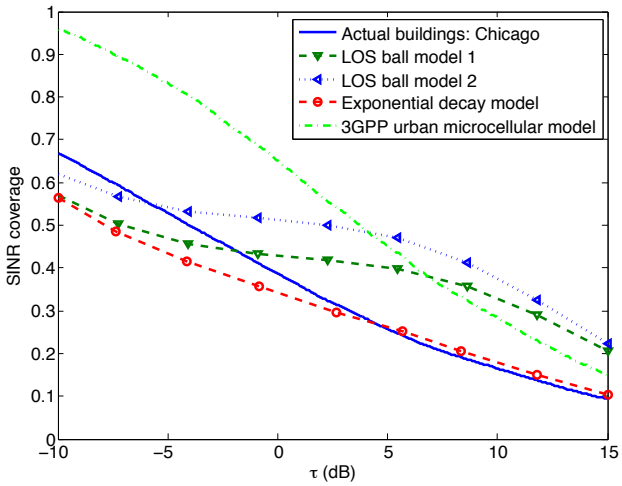

(b) Chicago

Fig. 5: Comparison of blockage models, $\mu = 30/\text{km}^2$

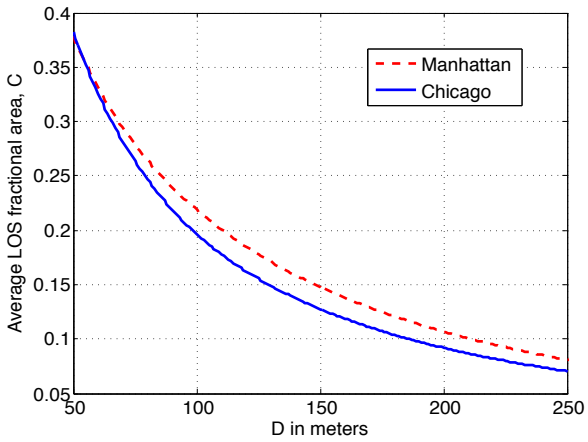

Fig. 6: Average LOS fractional area in a ball of radius D, obtained using actual building locations

radius D centered at several outdoor user locations in the Manhattan and Chicago regions. Note that the LOS fractional area in a ball of radius D is the ratio of LOS area in that ball to $\pi \mathrm{D}^2$. Fig. 6 shows empirical estimates of C as a function of D, averaged over 1000 user drops. Since each (C, D) pair is a unique characterisitic of the region under consideration, any such pair could form a plausible blockage model. However, by equation (8), choosing smaller values of D we loose more information about LOS links with link distances greater than D. Fig. 7 shows that choosing D in the range $150 - 250$ m gives reasonable estimates of SINR coverage. This figure also shows the robustness of the blockage model over different BS densities. Further, Fig. 8 shows that the blockage model fits the SINR coverage even at the lower mmWave frequency band at 28 GHz, which is expected since the blockage parameters (C, D) are only dependent on the building geometry and independent of the channel model. Validation of this blockage model, with rate coverage being the comparison metric, is available in [16].

It would be interesting to study if these validation insights can be generalized over other urban regions as well, but irrespective of the outcome this simple model can atleast serve as a prototype real-world blockage scenario that can be used in the system capacity analysis of mmWave cellular networks, with the blockage parameters tailored to fit either the Manhattan or Chicago downtown regions[3].

V. Conclusion and Future Work

To the best of authors' knowledge, this is the first work to incorporate realistic outdoor urban blockage effects and demonstrate that even very dense mmWave cellular networks, operating at 73 GHz, tend to be noise-limited. These insights indicate that the sophisticated interference management techniques developed for today's cellular networks may not be necessary for a mmWave cellular network. However, if the network employs space division multiple access (SDMA) or multi-user multiple input multiple output (MU-MIMO), the number of users being served at a time and thus, the number of beams interfering with a typical service link would increase multiple times. It would be interesting to investigate whether the noise-limited behaviour of mmWave networks would still hold in these scenarios.

Acknowledgment

The authors would like to thank anonymous reviewers for their helpful suggestions and comments. The authors would also like to thank Tianyang Bai for helpful discussions on the blockage model in [17].

[3]Note that the blockage model assumes that outdoor NLOS channel model holds for all user-BS links, with BSs lying in the indoor/*rooftop* region.

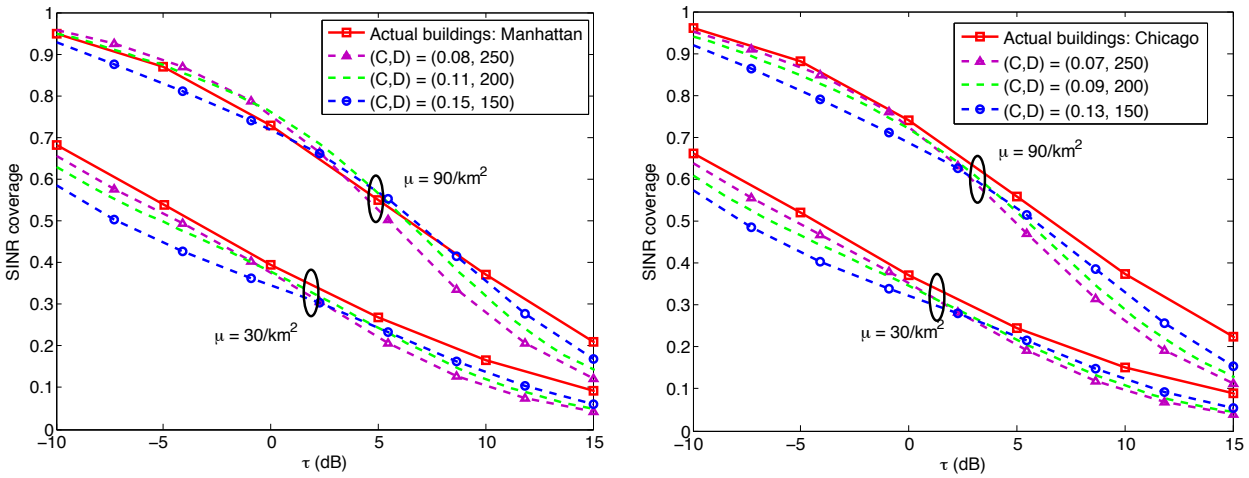

(a) Manhattan (b) Chicago

Fig. 7: Validation of the model in [16] for different BS densities and (C, D) pairs.

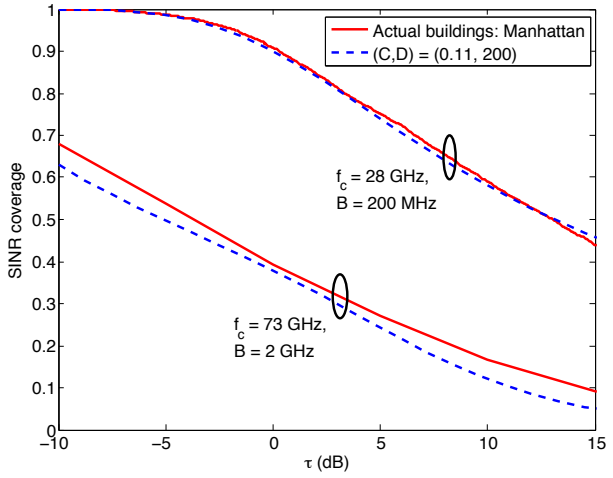

Fig. 8: Validation of the model in [16] over 28 GHz and 73 GHz mmWave frequency bands, $\mu = 30/\text{km}^2$.

REFERENCES

[1] Cisco, "Cisco Visual Networking Index: Global Mobile Data Traffic Forecast Update, 2012-2017," Whitepaper, available at: http://goo.gl/xxLT.

[2] T. Baykas *et al.*, "IEEE 802.15.3c: The first IEEE wireless standard for data rates over 1 Gb/s," *IEEE Commun. Mag.*, vol. 49, no. 7, pp. 114–121, July 2011.

[3] R. C. Daniels *et al.*, "60 GHz wireless: Up close and personal," *IEEE Microw. Mag.*, vol. 11, no. 7, pp. 44–50, Dec. 2010.

[4] Z. Pi and F. Khan, "An introduction to millimeter-wave mobile broadband systems," *IEEE Commun. Mag.*, vol. 49, no. 6, pp. 101–107, Jun. 2011.

[5] T. Rappaport *et al.*, "Millimeter wave mobile communications for 5G cellular: It will work!" *IEEE Access*, vol. 1, pp. 335–349, May 2013.

[6] Y. Azar *et al.*, "28 GHz propagation measurements for outdoor cellular communications using steerable beam antennas in New York City," *IEEE ICC*, pp. 5143–5147, Jun. 2013.

[7] T. S. Rappaport *et al.*, "38 GHz and 60 GHz angle-dependent propagation for cellular and peer-to-peer wireless communications," *IEEE ICC*, pp. 4568–4573, Jun. 2012.

[8] W. Roh *et al.*, "Millimeter-wave beamforming as an enabling technology for 5G cellular communications: theoretical feasibility and prototype results," *IEEE Commun. Mag.*, vol. 52, no. 2, pp. 106–113, Feb. 2014.

[9] S. Rangan, T. S. Rappaport, and E. Erkip, "Millimeter wave cellular wireless networks: Potentials and challenges," *Proc. IEEE*, vol. 102, no. 3, pp. 366–385, March 2014.

[10] M. R. Akdeniz *et al.*, "Millimeter wave channel modeling and cellular capacity evaluation," *IEEE J. Sel. Areas Commun.*, vol. 32, no. 6, pp. 1164–1179, June 2014.

[11] A. Ghosh *et al.*, "Millimeter wave enhanced local area systems: A high data rate approach for future wireless networks," *IEEE J. Sel. Areas Commun.*, vol. 32, no. 6, pp. 1152–1163, June 2014.

[12] T. Rappaport, J. N. Murdock, and F. Gutierrez, "State of art in 60 GHz integrated circuits and systems for wireless communication," *Proc. IEEE*, vol. 99, no. 8, pp. 1390–1436, Aug. 2011.

[13] S. Rajagopal *et al.*, "Antenna array design for multi-Gbps mmwave mobile broadband communication," *IEEE Globecom*, pp. 1–6, Dec. 2011.

[14] T. Bai and R. W. Heath Jr., "Coverage analysis for millimeter wave cellular networks with blockage effects," *IEEE GlobalSIP*, pp. 727–730, Dec. 2013.

[15] ——, "Coverage and rate analysis for millimeter wave cellular networks," *IEEE Trans. Wireless Commun.*, 2014, submitted. [Online]. Available: http://arxiv.org/abs/1402.6430

[16] S. Singh, M. N. Kulkarni, A. Ghosh, and J. G. Andrews, "Tractable model for rate in self-backhauled millimeter wave cellular networks," *IEEE J. Sel. Areas Commun.*, July 2014, submitted. [Online]. Available: http://arxiv.org/abs/1407.5537

[17] T. Bai, R. Vaze, and R. W. Heath Jr., "Analysis of blockage effects on urban cellular networks," *IEEE Trans. Wireless Commun.*, vol. PP, no. 99, Jun. 2014.

[18] F. Baccelli and B. Blaszczyszyn, *Stochastic Geometry and Wireless Networks, Volume II – Applications*. NOW: Foundations and Trends in Networking, 2009.

[19] The City of New York, "New York building perimeter data," Online, available at: http://tinyurl.com/khlo69r.

[20] The City of Chicago, "Chicago building perimeter data," Online, available at: http://tinyurl.com/mccksq4.

[21] M. N. Kulkarni, *MATLAB code for converting building location data from shapefiles to MAT files*, August 2014. [Online]. Available: http://tinyurl.com/omplkm4

[22] S. Singh, H. S. Dhillon, and J. G. Andrews, "Offloading in heterogeneous networks: Modeling, analysis, and design insights," *IEEE Trans. Wireless Commun.*, vol. 12, no. 5, pp. 2484–2497, May 2013.

[23] 3GPP, "Evolved Universal Terrestrial Radio Access (E-UTRA); Further advancements for E-UTRA physical layer aspects (Release 9)," TR 36.814, 2010.